

Anesthesia and surgery induce changes in endogenous brain protective protein (RNF146) and delirium-like behavior in aged rats

Yubo Gao^{1,2#}, Xu Han^{1,3#}, Xiuhua Li^{1,3#}, Shaling Tang^{1,3}, Chun Zhang³, Xiaoxia Yang^{1,2}, Majid Alhomrani⁴, Abdulhakeem S. Alamri⁴, Ghulam Nabi⁵ and Xinli Ni¹✉

¹Department of Anesthesiology, General Hospital of Ningxia Medical University, Yinchuan, Ningxia, 750004, China; ²Department of Anesthesia and Perioperative Medicine, General Hospital of Ningxia Medical University, Yinchuan, Ningxia, 750004, China; ³Ningxia Key Laboratory of Cerebrocranial Diseases, Ningxia Medical University, Yinchuan, Ningxia, 750004, China; ⁴Department of Clinical Laboratory Sciences, The Faculty of Applied Medical Sciences, Taif University, Taif, Saudi Arabia; ⁵Institute of Nature Conservation, Polish Academy of Sciences, Kraków, 31120, Poland

Background: Postoperative delirium (POD) is a common complication after anesthesia and surgery, especially in the elderly. RNF146 has neuroprotective effects in cerebral ischemia, hypoxia, and chronic neurological diseases. However, whether RNF146 expression is related to the occurrence and development of POD remains unclear. Therefore, in this study, we aimed to determine whether RNF146 is involved in the occurrence of POD. **Methods:** (Sprague-Dawley) male rats (18 months old) were splenectomized under sevoflurane anesthesia. The cognitive function of rats at 1, 3, and 7 d after anesthesia and surgery was evaluated. Changes in the expression of neuroinflammatory cytokines, IL-6 and IL-10, and RNF146 were measured in the hippocampus in both control group (con) and anesthesia (AS) group. We examined cognitive outcomes and expression of inflammatory factors and RNF146 in con and AS mice using cluster analysis. **Results:** The cognitive ability and mobility of rats after anesthesia and surgery at day 1, 3, and 7 decreased, especially at day 3. Similarly, the expression of neuroinflammatory factors and RNF146 increased after anesthesia and surgery at day 1, 3, and 7, and the increase was highest at day 3. The clustering and correlation analysis of RNF146 expression in the hippocampi of elderly rats revealed a correlation between POD and neuroinflammation resulting from anesthesia and surgery. **Conclusion:** Anesthesia and surgery can lead to POD and neuroinflammation. The expression of RNF146 correlates with delirium and neuroinflammation caused by anesthesia and surgery.

Keywords: RNF146, anesthesia, surgery, postoperative delirium, hippocampus, neuroinflammation

Received: 25 April, 2023; **revised:** 24 May, 2023; **accepted:** 24 May, 2023; **available on-line:** 26 October, 2023

✉e-mail: xinlini6@nyfy.com.cn

#Equal contribution

Acknowledgements of Financial Support: This study was supported by the Key Research & Developing Program of Ningxia Hui Autonomous Region (2021BEG02036) and the Ningxia Natural Science Foundation Project (2020AAC03218).

Abbreviations: ANOVA, One-way analysis of variance; IL-1, Interleukin 10; IL-6, Interleukin 6; POD, Postoperative delirium

INTRODUCTION

With the progress of modern medicine and the aging of the population, the number of elderly patients under-

going surgery and anesthesia is increasing (H *et al.*, 2017; Lin *et al.*, 2020). Postoperative delirium (POD) is a common complication of anesthesia and surgery in elderly patients. POD is characterized by mild cognitive impairment, impaired memory, decreased ability to process information, and reduced attention accompanied by a series of negative outcomes, including changes in mood, personality, and loss of labor ability (Evered *et al.*, 2018). Having POD may result in increased morbidity and mortality, deteriorating quality of life, and causing other physical and psychological diseases, which negatively affect social stability (Carr *et al.*, 2018; Deiner *et al.*, 2017). A study reported that patients with POD were nearly twice as likely to die within 1 year within 3 months of surgery compared with patients without POD (Fodale *et al.*, 2010). According to the International Postoperative Delirium Study, the incidence of POD in elderly patients (>60 years old) is approximately 25.8% within 7 days of surgery and 10% within 3 months of surgery (Moller *et al.*, 1998). The incidence of POD within 3 months and 1 year after surgery is approximately 29% and 33.6%, respectively (Deiner *et al.*, 2017; Liu *et al.*, 2022). However, the mechanism of POD is unclear. POD occurs due to the combined action of susceptibility and predisposing factors, and aging is the only independent risk factor for the occurrence of POD (Evered *et al.*, 2018). The pathogenesis of POD is believed to be mainly caused by central nervous system inflammation (Feng *et al.*, 2017), oxidative stress (Chen *et al.*, 2020), dysregulations of the cholinergic system (Zuo *et al.*, 2018), increased neuronal apoptosis (Zhang *et al.*, 2020), and decreased neuronal regeneration and synaptic plasticity caused by amyloid deposition (Evered *et al.*, 2018). However, neuroinflammation is an important pathological basis for the occurrence of POD (Li *et al.*, 2022).

The E3 ubiquitin ligase RNF146 is present in the brain, spleen, heart, kidney, and testis (Matsumoto *et al.*, 2017). Neuronal cytoplasm mainly expresses RNF146 at a relatively high level in the cortex and hippocampus (Yang *et al.*, 2017). Studies have confirmed that RNF146 has a neuroprotective effect in cerebral ischemia, hypoxia, and chronic nervous system diseases (Kim *et al.*, 2017; Mu *et al.*, 2020) and mediates DNA damage repair through PAR-dependent ubiquitination to degrade PAR-mediated proteins (Andrabi *et al.*, 2011; Koo *et al.*, 2018). Cells overexpressing RNF146 exhibited higher survival rates after γ -irradiation (Andrabi *et al.*, 2011; Bensih *et al.*, 2023). *In vitro* and *in vivo* experiments have revealed

that RNF146 expression in nerve cells is significantly increased after exposure to low-dose *n*-methyl-d-aspartic acid (NMDA) receptor and sublethal glucose-oxygen deprivation or transient bilateral common carotid artery occlusion in mice, protecting nerve cells from injury (Belayev *et al.*, 2017; Mu *et al.*, 2020). The presence of higher RNF146 expression in the brains of patients with early Alzheimer's disease supports a neuroprotective role for RNF146 (von Rotz *et al.*, 2005). The occurrence and clinical manifestations of POD are similar to neuroinflammation-related degenerative diseases, such as Alzheimer's disease (Belayev *et al.*, 2017; Evered *et al.*, 2018). However, whether RNF146 is involved in the occurrence and development of POD is unknown. In this study, elderly rats were used to induce delirium-like behavior during anesthesia and surgery to evaluate changes in RNF146 expression in the occurrence of POD. The purpose of this paper is to investigate the changes of RNF146 expression during POD development, whether RNF146 can be a biomarker of POD development, and to improve new insights for studying the pathogenesis, treatment, and prevention of POD.

MATERIALS AND METHODS

The animal program was approved by the Animal Care and Use Committee of Ningxia Medical University Medical Center. All animal experiments were conducted following the National Institutes of Health Guidelines for the Care and Utilization of Laboratory Animals (No. 2016-124), revised in 2016.

Animals

A total of 72 healthy male SPF (Specific pathogen Free) SD rats, aged 18–20 months and weighing 450–600 g, were provided by the Laboratory Animal Center of Ningxia Medical University (IACUC Animal Use License number: SCXK (Ning) 2020-0001). The rats were randomly divided into six groups (12 animals in each group): con group 1, 3, and 7 d without exposure to anesthesia and AS group 1, 3, and 7 d after anesthesia and surgical intervention. Each cage, measuring 27.94 cm×15.24 cm×11.43 cm, contained 3–4 animals under a 12-h light–dark cycle. The rats were provided free access to food and water.

Anesthesia and Surgery

Splenectomy was performed under anesthesia with sevoflurane in the AS group. In brief, rats were anesthetized in an airtight chamber prefilled with 3% sevoflurane in 100% O₂. Anesthesia was induced by continuous inhalation of 3% sevoflurane in 100% O₂ at a rate of 1.5 L/min. As soon as the correct reflex disappeared, the rats breathed spontaneously after being fixed on the operating table. In order to maintain the depth of anesthesia, rats were given 100% pure oxygen mixed with 3% sevoflurane. Splenectomy was performed in the AS group according to the methods described in the literature (Kong *et al.*, 2017; Wang *et al.*, 2017). The operation was performed on a heating table and the temperature was maintained at 37°C. Skin disinfection was performed routinely. First, an incision of 1 cm was made, and a surgical field was created. The spleen was bluntly separated from the surrounding tissue. Then the blood vessel was ligated with 6-0 thread, and the distal blood vessel was cut after the spleen was taken out. Abdominal muscles and skin were sutured with 4-0 silk thread. The incision

was locally infiltrated with ropivacaine (1%, 1 mL), and erythromycin ointment was applied to the incision. The rats were kept at 37°C±0.5°C from anesthesia until they woke up. The entire operation was completed in 30 min, and a sine individual performed all the surgical operations. The rats in the con group were placed in the air-containing induction chamber for 30 min.

Morris water maze test

The Morris water maze (MWM) test of spatial memory and cognitive ability was performed in splenectomized rats. The MWM consists of a circular pool of 120 cm in diameter and 50 cm in height. The pool was divided into four quadrants. A circular platform with a diameter of 15 cm was fixed in the middle of the second quadrant. The platform was immersed 1 cm underwater, with a water temperature of 22°C±2°C. A camera was placed above the maze to record the rats' movements. The test included the following: (1) Positioning navigation experiment: The experiment was conducted at the same time every day, once a day for 5 consecutive days. The time for rats to find the platform was recorded as escape latency. The automatic camera system and computer analysis and processing system recorded escape latency. If the rat could not find the platform within 60 s after entering the water, it was led to the platform and allowed to stay on it for 15 s to guide its spatial learning and memory. In such cases, the escape incubation period was recorded as 100 s; (2) Space exploration experiment: The platform was removed on the second day after the positioning navigation experiment, and the rat was placed into the water facing the pool wall at the entry point of 1/2 arc in the fourth quadrant. The computer recorded the time it took the rat to reach the original platform position, the number of times it crossed the platform position, and the total swimming distance within 60 s. The samples were collected after the behavioral experiment.

IntelliCage test (automated IntelliCage testing)

The IntelliCage test (TSE Systems GmbH, Germany; <http://www.newbehavior.com>) assessed spontaneous behavior and spatial learning in rats raised in groups. After surgery, the rats in each experimental group were put in the IntelliCage box before adding water and feed and changing the padding regularly. A miniature signal transceiver was injected into the neck of the rats (used to record activity) (Wu *et al.*, 2017). The labels of each group of rats injected were input in the IntelliCage test software (IntelliCage plus). The experimental test could detect when the rats entered the corner, and the system recorded it as a "visit". Two water bottles were placed in each corner, and the system records a "nose-poke" when rats touch their noses. When a rat licks a water bottle for a drink, the system records it as a lick. The IntelliCage test was designed in four stages: (1) Free exploration: The number of corner visits and nose contacts of each rat was recorded to assess the ability of the rat to adapt to the new environment for 3 d. (2) Nose-poke learning: The times of corner visits and a nasal touch of each rat were recorded to evaluate the learning and memory ability of the rat for 5 d. POD modeling was performed after nose contact learning. (3) Position learning: The correct access ratio of each rat was recorded to evaluate the spatial position learning ability for 3 d. After the end of the learning behavior, all rats had access to all corners and vial vents. (4) Position reversal learning: the diagonal corner of the "correct" area in the previous spatial position learning stage was defined as "correct"

and the rest as “wrong.” The number of times each rat visited the correct corner was recorded to evaluate the learning ability of spatial position for 3 d.

Nesting test

The nesting experiment is used to evaluate the behavior and habits of rats. Before the experiment, each rat was placed in a new sterilized cage, facial tissue was added (the thickness of the cage was ~1.5 cm), and 10 pieces of clean, unscented tissue paper were placed in the cage (close to the side wall of the cage, and not right below the water bottle). The rectangular paper measured 10×6 cm. After the rats were put in, the cage was covered, and the room lights were turned off. The experiment generally started from 16:00 to 18:00, and all rats were placed within 1 h to reduce experimental errors. The nesting situation of the rats was scored at 24 h.

Score with reference to the literature: 1 = no obvious bite marks on the paper; 2 = partial shredding of the paper; 3 = scrap most of the paper; 4 points = flat nest can be identified; 5 = perfect nest. The experiment was double-blind, scored by more than three trained experimenters, and each experimenter's rating of a rat was evenly divided into the rat's nesting score.

Western blotting

After MWM, six animals in each group were injected with cold PBS (phosphate buffered saline) and normal saline through the cardiac vein under deep anesthesia, and their brains were quickly removed. Brain tissue was homogenized in a mixture of RIPA lysis buffers, phosphatase, and protease inhibitors and incubated in ice for 30 min. The lysates were then ultrasonicated and centrifuged at 13000×g at 4°C for 30 min. Protein samples were quantified using a BCA protein determination kit (Thermo Scientific, Waltham, MA, USA) and concentrations were determined using a spectrophotometer (MULTISKAN MK3, Thermo Scientific). Subsequently, the samples were mixed with 5× sample buffer, balanced with double distilled water, and heated at 100°C for 5 min. An equal amount of protein in each sample was separated by sodium dodecyl sulfate-polyacrylamide gel electrophoresis on a 10% gel and then electrophoretically transferred to a polyvinylidene fluoride membrane (Bio-Rad, Hercules, CA, USA). Blocking was performed with 10% skim milk in Tris-buffered saline and Tween-20 (0.1%) (TBST) for 2 h. Then the membranes were immunoblotted with primary antibodies (RNF146, 1:1000, ab2736529, Invitrogen, USA; IL-6, 1:1000, ab9324, Abcam, USA; IL-10, 1:1000, DF6894, Affinity Biosciences, China) overnight. After being incubated with secondary antibody (1:5000, anti-rabbit antibody, ab150077, Abcam), signal detection was performed by Odyssey infrared laser imaging system, followed by gray intensity analysis.

RT-PCR

Total RNA of the hippocampus was extracted using TRIzol reagent according to the manufacturer's protocol (TransGen Biotech). The reaction system was configured with a real-time quantitative PCR kit using 2 μL DNA as a template, and the reaction was amplified *in vitro* by quantitative PCR. The expression level of miR-RNF146 (internal reference GAPDH) was analyzed using the 2^{-ΔΔCT} method. The primers used for real-time fluorescent quantitative PCR are shown in Table 1. The primers and sequencing reactions were sent to Shanghai Sangong Bioengineering Co., Ltd.

ELISA

The hippocampus was homogenized with an extraction buffer containing 5 mol/L guanidine hydrochloride in 50 mmol/L Tris-HCl and a protease inhibitor cocktail containing a serine protease inhibitor AEBSF, according to the manufacturer's instructions (Jiang Lai, China). In brief, the samples were centrifuged at 16000×g for 20 min at 4°C and the supernatant was diluted from 1:2 to 1:10, added to ELISA plates coated with anti-mouse IL-6 or IL-10 antibody, respectively, and then incubated for 2 h at RT. After the samples were washed, they were incubated with 100 μL of IL-6 or IL-10 detection antibody for 1 h at RT, washed, and incubated with 100 μL of horseradish peroxidase labeled anti-rabbit antibody for 30 min at RT. Then the stop solution was added, and absorbance was measured at 450 nm with a spectrophotometer (Nanodrop2000C, ThermoScientific). The protein samples were quantified using an ELISA assay kit (Jiang Lai, China) and the concentration was determined with a spectrophotometer. The concentration of IL-6 and IL-10 was expressed in pg/mg tissues.

Immunofluorescence

All six animals in each group were deeply anesthetized with 5% chloral hydrate, infused with normal saline through the cardiac vein, and bled simultaneously in the right atrium. The animals were given 4% paraformaldehyde in 0.1 mol/L phosphate buffer (pH of 7.4) 24 h after MWM. The brain was removed and stored overnight in 4% paraformaldehyde at 4°C. Continuous 30-μm coronal sections were cut from the frozen samples using a cryoslicer (Thermo Scientific HM430, Microm, Germany). The frozen sections were warmed at RT for 30 min and washed three times with TBS for 5 min each. The sections were blocked with 5% BSA and incubated with antibodies overnight at 4°C (RNF146, 1:200, ab2736529 Invitrogen, USA; IL-6, 1:200, ab9324, Abcam, USA; IL-10, 1:200, DF6894, Affinity Biosciences, China). Then the samples were washed three times with TBS, incubated with CY3-labeled goat anti-rat IgG (H+L) (1<500) at RT for 3 h, and washed with TBS three times for 10 min each. The tablets were sealed with anti-fluorescence quenching tablets containing DAPI (4',6-diamidino-2-phenylindole) and photographed using a fluorescence microscope (The Chongqing Optical Instrument Factory). Average fluorescence intensity was analyzed using the image analysis software ImageJ1.48. The coronal plane of brain tissue in the hippocampus was included in the samples of three rats in each group for observation and analysis. The middle piece was selected to be photographed, and the average fluorescence intensity of CA1 in the hippocampus of each sample was calculated to compare differences between groups.

Statistical analysis

Data were analyzed using the SPSS21.0 software (SPSS Inc., Chicago, IL, USA). Measurement data were expressed as mean ± standard deviation (mean ± S.D.).

Table 1. Primers used for real-time fluorescent quantitative PCR

Primer name	Primer sequence (5'-3')
RNF146-sense	ATAAGAAGGCGAGTGAGACC
RNF146-anti	AGGGCAGACTGACTGGATGA
GAPDH-sense	ACAACCTTGGCATTGTGGAA
GAPDH-anti	GATGCAGGGATGATGTTCTG

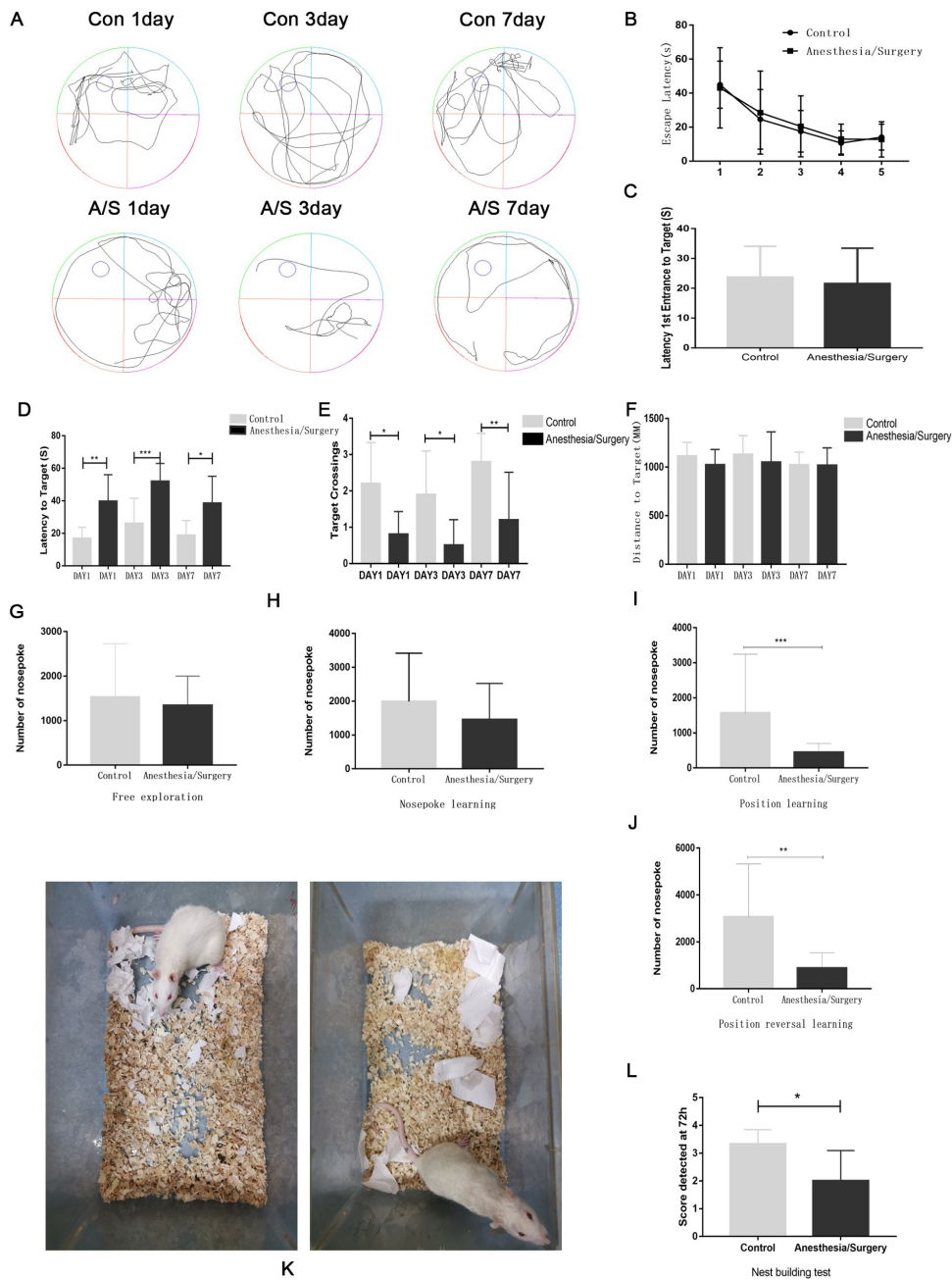


Figure 1. Behavioral changes in aged rats after anesthesia and surgery

One-way analysis of variance (ANOVA) was used to compare means between groups, SNK-q test (Student-Newman-Keuls) was used for pairwise comparison, and repeated measures analysis of variance was used for the water maze test. $P < 0.05$ was considered statistically significant, and the test level of homogeneity of variance was 0.1.

RESULTS

Learning and memory ability before anesthesia and surgery

The water maze and IntelliCage experiments were conducted to evaluate the learning and spatial memory ability of rats before anesthesia and surgery. The repre-

sentative tracking's of rats' movement in the test session were shown in Fig. 1A. During the positioning navigation stage of the water maze experiment, no statistically significant differences were observed in the learning abilities of the rats in the AS and con groups (Fig. 1B, 1C). During the free exploration and nose-poke learning stage in the IntelliCage system, no statistically significant differences were observed in the total number of corner visits and licks between the AS and con groups (Fig. 1G, 1H). The results showed that the two groups' cognitive learning ability was the same under normal conditions. The test was performed at the end of spatial learning on day 5. The learning ability level of the two groups was the same, with no statistically significant difference (Fig. 1B). The influence of individual differences and groups on the experiment was excluded.

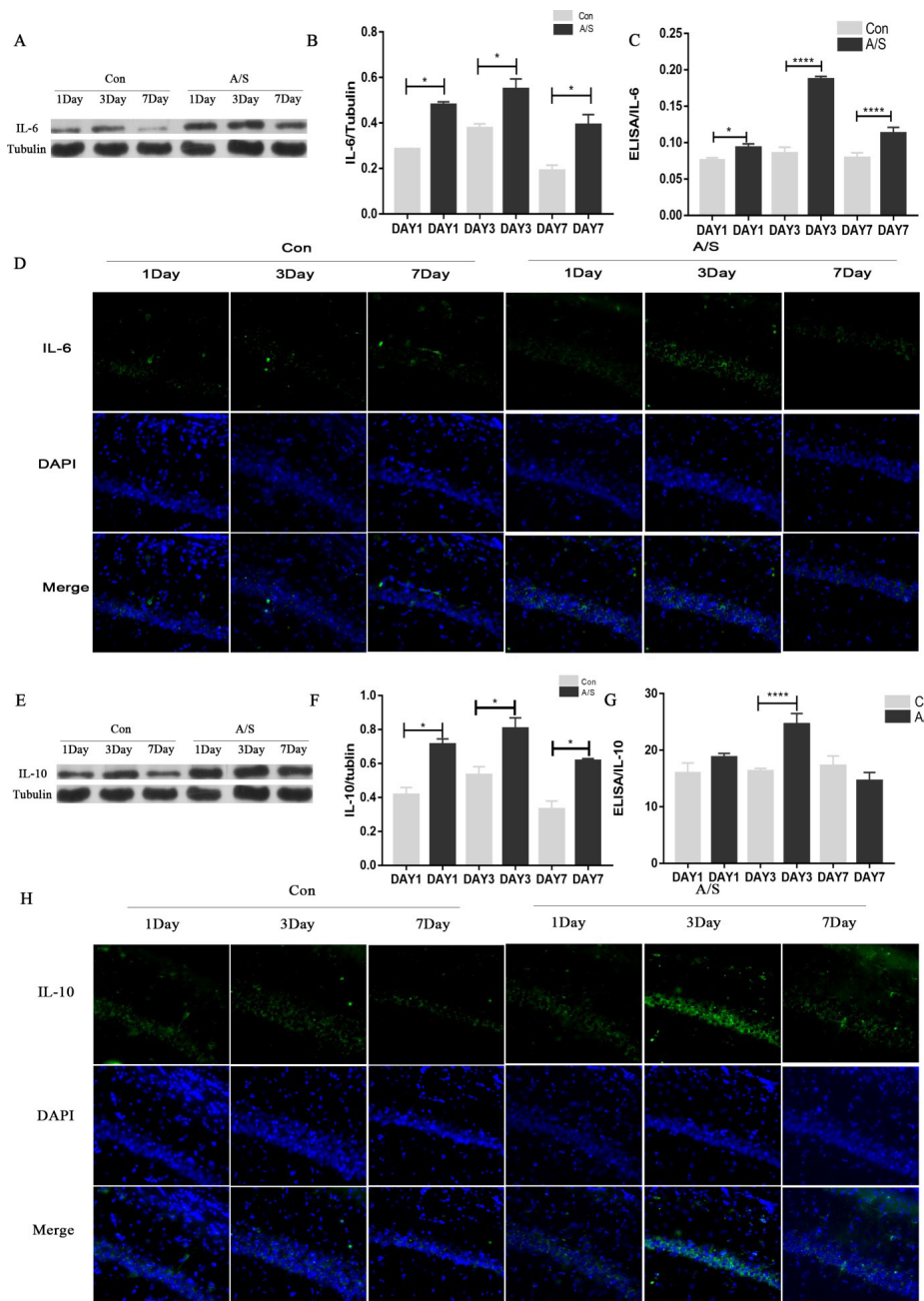


Figure 2. Neuroinflammatory response was induced in aged rats after anesthesia and surgery

Anesthesia and surgery induced decrease in learning and memory and decreased purposeful behavior.

The rats underwent behavioral evaluation after anesthesia and surgery. In the water maze experiment, compared with the con group, the escape latency of rats 1, 3, and 7 d after surgery in the AS group was longer (Fig. 1D) and the number of platform crossings was smaller (Fig. 1E). In the AS group, the escape latency time was the longest (Fig. 1D) and the number of platform crossings was the lowest (Fig. 1E) on day 3 after surgery compared with days 1 and 7 after surgery, whereas the parameters in the con group were not statistically different (Fig. 1F). During the spatial learning exploration in the IntelliCage experiment, the number of correct accesses and licks was significantly lower in the AS group than the con group (Fig. 1I), suggesting that learning and spatial memory decreased within 3 d after

the operation. In the inverse spatial learning exploration stage, the correct visits and licks of the AS group were significantly lower than those of the con group (Fig. 1J), suggesting that the learning and spatial memory ability of rats decreased within 7 d after anesthesia and operation. At the end of the experiment, the three groups of rats did not lose weight, excluding the interference of post-operative pain.

The nesting experiment was performed at the end of the water maze experiment 3 d after surgery. The con group rats tore most of the pieces of paper and the pieces were orderly stacked to build a complete nest, resulting in high nesting scores. Rats in the AS group tore a few pieces of paper, stacked a few pieces of paper or did not stack to build nests, with only embryonic nests or no nests, and the nesting scores decreased significantly (Fig. 1K). Compared with the con group, the difference

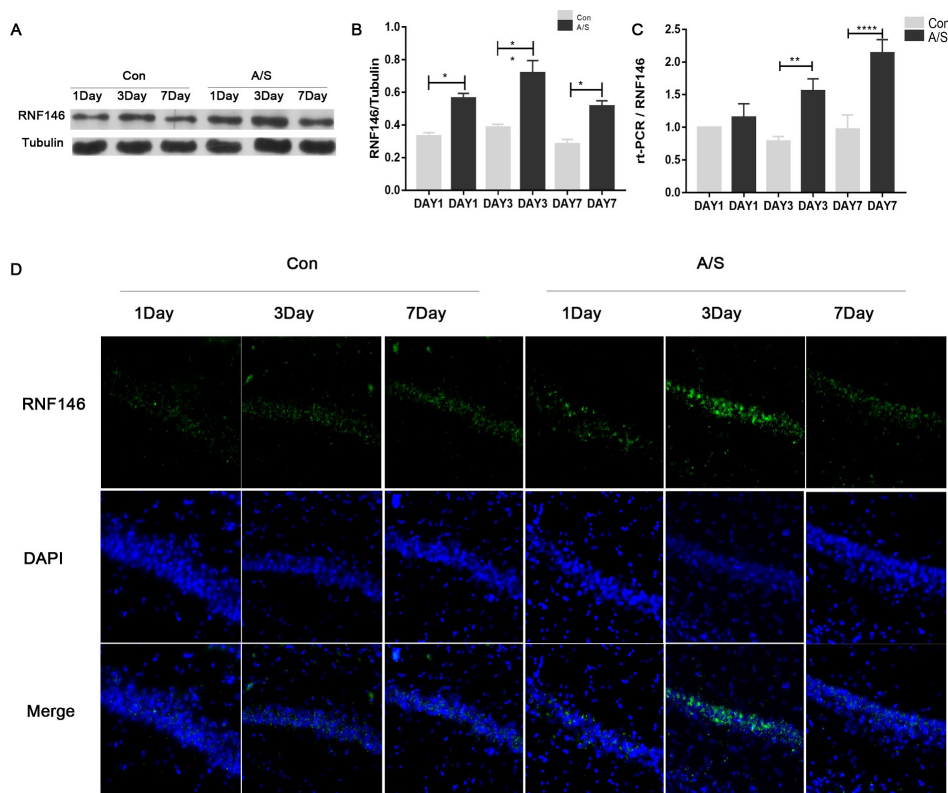


Figure 3 Expression of RNF146 in aged rats after anesthesia and surgery

was statistically significant (Fig. 1L). The results indicated that the executive function and daily activity ability of rats undergoing anesthesia and operation decreased.

Anesthesia and surgery induced changes in the levels of neuroinflammatory factors

To evaluate central nervous system inflammation in rats after anesthesia and surgery, we tested the expression of IL6 and IL-10 in the CA1 region of the hippocampus (Fig. 2A, 2E). Results from western blot analysis and immunofluorescence showed that the expression and fluorescence intensity of IL6 and IL-10 in the hippocampus of the AS group increased at 1, 3, and 7 d after surgery compared with those of the con group (Fig. 2B, 2D, 2F, 2H). In the AS group, the protein content and fluorescence intensity of IL-6 and IL-10 at 3 d after surgery were higher than those at 1 and 7 d after surgery (Fig. 2B, 2D, 2F, 2H). ELISA results were consistent with western blot and immunofluorescence tests (Fig. 2C, 2G).

Anesthesia and surgery induced changes in RNF146 expression

We detected changes in the expression of RNF146 in CA1 region after anesthesia and surgery (Fig. 3A). It shows that compared with the con group, the protein expression and fluorescence intensity of RNF146 in the hippocampus of the AS group increased 1, 3, and 7 d after surgery (Fig. 3B, 3D). Compared within the AS group, the protein expression and fluorescence intensity of RNF146 in the hippocampus of the AS group at 3 d after surgery were higher than those at 1 and 7 d after surgery. These results confirmed the high expression of RNF146 protein content and fluorescence intensity in neurons induced by anesthesia

and surgical stimulation in aged rats. The results of RT-PCR experiment showed that compared with the con group, the expression of miR-RNF146 in the hippocampus of the AS group was higher at days 1, 3, and 7 (Fig. 3C). In the AS group, miR-RNF146 in the hippocampi of rats 1 day after surgery was lower than that in rats 3 d after surgery ($p < 0.05$), and miR-RNF146 in the hippocampal region of rats 3 d after surgery was lower than that in rats 7 d after surgery (Fig. 3C).

Correlation analysis of RNF146 with behavioral and neuroinflammatory factors

Experimental data parameters were analyzed by hierarchical clustering and correlation testing. Figure 4 shows the correlation between RNF146, inflammatory cytokines IL-6, IL-10, and behavioral data. The relative expression of RNF146 was positively correlated with the relative expression of inflammatory factors IL-6 and IL-10 (Fig. 4) and was negatively correlated with the escape latency in the water maze experiment, which showed significant correlation ($p < 0.05$). It is indicating that after anesthesia/surgery, the expression of endogenous brain protective protein RNF146 is associated with hippocampus-dependent cognitive impairment and central nervous system inflammation. The expression of RNF146 was negatively correlated with the number of times that rats crossed the platform in the water maze, again demonstrating its correlation with hippocampus-dependent cognition. In addition, the correlation coefficients between RNF146 expression and cognition-related indicators in the IntelliCage system were concentrated between 0.1 and 0.4, but the correlation was not significant.

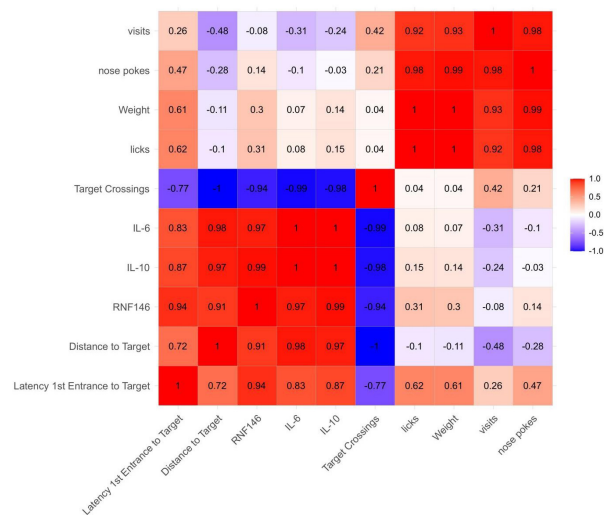


Figure 4. Heat maps of RNF146 and parameters of anesthesia and surgical induction in rats

DISCUSSION

The study investigated the involvement of RNF146 induced by anesthesia and surgery in aged rats and dissected the molecular mechanism underlying this regulation. Ho Chul Kang stated that RNF146 regulates cell survival and DNA repair by ubiquitinating PAR and blocking AIF nuclear translocation to inhibit parthanatos cell death (Kang *et al.*, 2011). In the oxygen and glucose deprivation/reoxygenation (OGD/R) model, NPD1 induces activation of the Wnt/ β -catenin pathway through upregulation of RNF146, enhanced cell survival, decreased oxidative stress markers, and a lower level of autophagy (Mu *et al.*, 2020). With reference to Ismail Nurul Iman and others (Iman *et al.*, 2021), this study combined the IntelliCage experiment and the traditional water maze experiment and nesting evaluation of elderly rats to assess learning and memory and ability to care for themselves. The findings revealed that learning and memory and ability for daily living of aged rats after anesthesia decreased on days 1, 3, and 7 after surgery, and the abnormal neurobehavioral function recovered on day 7 after surgery. Clinical evidence also shows that POD occurs mostly within 24–72 h after surgery. Most patients heal within 1 week, but some patients may develop long-term cognitive dysfunction. Animal experiment studies have shown that the appropriate time period for observing delirium-like behavior changes in rodents after anesthesia is 24–48 h, and neurobehavioral changes are the most obvious at this time. These results are consistent with our findings. Neuroinflammation causes delirium after general anesthesia in rodents (Cao *et al.*, 2010; Dong *et al.*, 2016). In animal models, the synthesis and release of proinflammatory factors can damage nerve formation and synaptic plasticity and nerve repair function (Belarbi *et al.*, 2012; Liu *et al.*, 2018). Studies have shown that anesthesia and surgery increase the level of IL-6 in the hippocampi of aged wild-type mice, resulting in cognitive dysfunction in aged mice. The use of the IL-6 antibody can improve cognitive dysfunction after peripheral trauma in aged wild-type mice. In addition, anesthesia did not affect the level of IL-6 in the hippocampi of IL-6 gene knockout rats, nor did it lead to cognitive impairment in aged IL-6 gene knockout rats, suggesting that the increase of IL-6 may be involved in

the cognitive dysfunction caused by anesthesia surgery (Dong *et al.*, 2016; Naveed *et al.*, 2022; Muhammad AS *et al.*, 2023; Waseem *et al.*, 2023). After anesthesia surgery, aged rats exhibited impaired spatial memory and significantly higher expression of inflammatory factor IL-6 within 1 and 3 d after surgery. Spatial memory is improved, and the expression of inflammatory factors is downregulated 7 d after surgery (Cao *et al.*, 2010). Studies have indicated that IL-10 is not only closely related to autoimmune diseases and infectious diseases, but also has neuroprotective effects in cerebral ischemia, hypoxia, and chronic nervous system diseases (Morris *et al.*, 2018; Sudheimer *et al.*, 2014; Wang *et al.*, 2019). Furthermore, in *in vitro* experiments, M2-type microglia produced IL-10 and TGF- β to reduce the neuronal cell damage caused by OGD, and this response was downregulated when the damage or pathogen was removed (Ahmad *et al.*, 2023; Zhao *et al.*, 2017). Li *et al.* reported that in the rat model of acute cerebral ischemia, IL-10 increased sharply 6 h after surgery, suggesting the activation of the anti-inflammatory system (Li *et al.*, 2001). In clinical studies, IL-10 in acute cerebral infarction began to rise at 24 h after surgery, reached a peak at 3 d after surgery, and then gradually decreased (van Exel *et al.*, 2002). IL-10 has similar biological activities in humans and mice (Moore *et al.*, 2001). In our study, the expressions of IL-6 and IL-10 in the hippocampi of aged rats at 1, 3, and 7 d after anesthesia were higher than that in the control group, and the expressions increased most significantly on day 3 after anesthesia. Our findings coincide with the results of other studies, suggesting that inflammatory and anti-inflammatory effects exist simultaneously in the nervous system after anesthesia and surgery.

RNF146, also known as Iduna, has two important functional regions in its N terminus: E3 ubiquitin ligase active region and PAR binding region, and the C3HC4 RING finger domain in amino acids 35–77 showed E3 ubiquitin ligase activity (Belayev *et al.*, 2017; Koo *et al.*, 2018). When glutamate excitatory toxicity, oxygen glucose deprivation, and other sublethal stimuli caused neuronal damage, RNF146 could recognize PARP1 to ubiquitinate and degrade axin/tankyrase through WWE domain-mediated PARP1, positively regulate Wnt/ β -catenin signaling pathway, and inhibit autophagy-induced death. It can reduce the excitatory toxicity of glutamate and damage of neurons induced by oxygen and sugar deprivation, and play a role in protecting neurons from damage (Mu *et al.*, 2020). In addition, RNF146 binds to apoptosis-inducing factor, a key death molecule in the parthanatos death pathway, and prevents the nuclear translocation of apoptosis-inducing factor in the mitochondria (Andrabi *et al.*, 2011). Thus, glutamate and NMDA receptor excitotoxicity-mediated cell parthanatos death is inhibited and brain protective effect is generated (Yang *et al.*, 2017). The Wnt signaling pathway plays an important role in POD. A study showed that treatment with 3.6% sevoflurane for 6 h inhibited the Wnt/ β -catenin signaling pathway, thereby increasing GSK-3 β and decreasing β -catenin. By inhibiting this pathway, sevoflurane downregulates annexin A1, thereby breaching the blood–brain barrier and inducing POD. However, it is unclear whether increasing the expression of RNF146 can activate the Wnt/ β -catenin pathway and increase the concentration of β -catenin, thus inhibiting the occurrence of POD (Hu *et al.*, 2016). However, our findings revealed that the expression of RNF146 in the hippocampi of aged rats increased 1, 3, and 7 d after surgical anesthesia, especially on day 3, when the increase was the most obvious. This change was consistent with

neurobehavioral changes and expression of neuroinflammatory factors IL-6 and IL-10 in the brain. Correlation analysis showed that the relative expression of RNF146 was positively correlated with the relative expression of inflammatory factors IL-6 and IL-10, as well as the escape latency in the water maze experiment, with the correlation coefficients being 0.90 and 0.99, respectively, and the correlation was significant.

RNF146 is an endogenous protective protein. When the body receives injury, RNF146 increases its reactivity and defends against external injury. Studies have confirmed this phenomenon. After exposure to low-dose NMDA and sublethal OGD or transient bilateral common carotid artery occlusion, the expression of RNF146 in mice nerve cells significantly increased to protect the nerve cells from injury. RNF146 may play the same role as anti-inflammatory factors such as IL-10 in the occurrence of POD.

CONCLUSION

Our findings reveal that after anesthesia and surgery, rat spatial learning and memory ability decreases and RNF146 expression increases and the level of IL-6 and IL-10 increases. Hierarchical cluster analysis showed that the expression of RNF146 was related to the degree of central nervous system inflammation and spatial learning and memory impairment. RNF146 may play a neuroprotective role similar to that of the anti-inflammatory factor IL-10. However, the mechanisms involved need to be investigated. In addition, the limitation of this study is that RNF146 was not knocked down or overexpressed in rats to verify the mechanism of action of RNF146 in POD. This will be a topic of research for the future.

Declarations

Data Sharing Statement. The datasets used and analysed during the current study are available from the corresponding author on reasonable request.

Ethics Approval and Consent to Participate. Rats were provided from the Animal Center of Ningxia Medical University (China) and all experiments were in accordance with the Regulations of Experimental Animal Administration issued by the State Committee of Science and Technology of China on May 2016.

Disclosure. The authors report no conflicts of interest in relation to this work.

REFERENCES

- Ahmad B, Muhammad Yousafzai A, Maria H, Khan AA, Aziz T, Alharbi M, Alsahamari A, Alasmari AF (2023) Curative effects of *Dianthus orientalis* against paracetamol triggered oxidative stress, hepatic and renal injuries in rabbit as an experimental model. *Separations* **10**: 182. <https://doi.org/10.3390/separations10030182>
- Andrabi SA, Kang HC, Haince JF, Lee YI, Zhang J, Chi Z, et al (2011) Iduna protects the brain from glutamate excitotoxicity and stroke by interfering with poly(ADP-ribose) polymer-induced cell death. *Nat Med* **17**: 692–699. <https://doi.org/10.1038/nm.2387>
- Andrabi SA, Kang HC, Haince JF, Lee YI, Zhang J, Chi Z, West AB, Koehler RC, Poirier GG, Dawson TM, Dawson VL (2011) Iduna protects the brain from glutamate excitotoxicity and stroke by interfering with poly(ADP-ribose) polymer-induced cell death. *Nature Med* **17**: 692–699. <https://doi.org/10.1038/nm.2387>
- Belarbi K, Jopson T, Tweedie D, Arellano C, Luo W, Greig NH, Rosi S (2012) TNF- α protein synthesis inhibitor restores neuronal function and reverses cognitive deficits induced by chronic neuroinflammation. *J Neuroinflammation* **9**: 23. <https://doi.org/10.1186/1742-2094-9-23>
- Belayev L, Mukherjee PK, Balaszczuk V, Calandria JM, Obenaus A, Khoutorova L, Hong SH, Bazan NG (2017) Neuroprotectin D1 upregulates Iduna expression and provides protection in cellular uncompensated oxidative stress and in experimental ischemic stroke. *Cell Death Differ* **24**: 1091–1099. <https://doi.org/10.1038/cdd.2017.55>
- Benish R, Sobia A, Nureen Z, Sohail A, Abid S, Najeeb U, Tariq A, Metab A, Abdulrahman A, Abdullah FA (2023) Evaluating the influence of Aloe barbadensis extracts on edema induced changes in C-reactive protein and interleukin-6 in albino rats through in vivo and in silico approaches. *Acta Biochim Pol*. Epub No: 6705. https://doi.org/10.18388/abp.2020_6705
- Bin W, Siyuan L, Xipeng C, Xinghui D, Jingzhu L, Ling W, Mingshan W, Yanlin B (2017) Blood-brain barrier disruption leads to postoperative cognitive dysfunction. *Curr Neurovasc Res* **14**: 359–367. <https://doi.org/10.2174/1567202614666171009105825>
- ChunLong Z, ChunMan W, Jin L, Ting S, JiangPing Z, XinRui H, Yi Z, HuaCheng L, QingQuan L, Han L (2018) Isoflurane anesthesia in aged mice and effects of A1 adenosine receptors on cognitive impairment. *CNS Neurosci Ther* **24**: 212–221. <https://doi.org/10.1111/cns.12794>
- Deiner S, Luo X, Lin HM, Sessler DI, Saager L, Sieber FE, Lee HB, Sano M, and the Dexlirium Writing Group; Jankowski C, Bergese SD, Candiotti K, Flaherty JH, Arora H, Shander A, Rock P (2017) Intraoperative infusion of dexmedetomidine for prevention of postoperative delirium and cognitive dysfunction in elderly patients undergoing major elective noncardiac surgery: a randomized clinical trial. *JAMA Surg* **152**: e171505. <https://doi.org/10.1001/jamasurg.2017.1505>
- Evered LA, Silbert BS (2018) Postoperative cognitive dysfunction and noncardiac surgery. *Anesth Analg* **127**: 496–505. <https://doi.org/10.1213/ane.0000000000003514>
- Feng X, Valdearcos M, Uchida Y, Lutrin D, Maze M, Koliwad SK (2017) Microglia mediate postoperative hippocampal inflammation and cognitive decline in mice. *JCI Insight* **2**: e91229. <https://doi.org/10.1172/jci.insight.91229>
- Fodale V, Santamaria LB, Schifilliti D, Mandal PK (2010) Anaesthetics and postoperative cognitive dysfunction: a pathological mechanism mimicking Alzheimer's disease. *Anaesthesia* **65**: 388395. <https://doi.org/10.1111/j.1365-2044.2010.06244.x>
- Iman IN, Yusof NAM, Talib UN, Ahmad NAZ, Noraziz A, Kumar J, Mehat MZ, Jayabalan N, Muthuraju S, Stefaniuk M, Kaczmarek L, Muzaimi M (2021) The IntelliCage system: a review of its utility as a novel behavioral platform for a rodent model of substance use disorder. *Front Behav Neurosci* **15**: 683780. <https://doi.org/10.3389/fnbeh.2021.683780>
- Jiqian Z, Shasha Z, Peipei J, Yuting H, Qingqing D, Qianyun Z, Pengfei W, Zhilai Y, Lei Z, Hu L, Guanghong X, Lijian C, Erwei G, Yunjiao Z, Longping W, Xuesheng L (2020) Graphene oxide improves postoperative cognitive dysfunction by maximally alleviating amyloid beta burden in mice. *Theranostics* **10**: 11908–11920. <https://doi.org/10.7150/thno.50616>
- Kim H, Ham S, Lee JY, Jo A, Lee GH, Lee YS, Cho M, Shin HM, Kim D, Pletnikova O, Troncoso JC, Shin JH, Lee YI, Lee Y (2017) Estrogen receptor activation contributes to RNF146 expression and neuroprotection in Parkinson's disease models. *Oncotarget* **8**: 106721–106739. <https://doi.org/10.18632/oncotarget.21828>
- Koo JH, Yoon H, Kim WJ, Cha D, Choi JM (2018) Cell-penetrating function of the Poly(ADP-Ribose) (PAR)-binding motif derived from the PAR-dependent E3 ubiquitin ligase iduna. *Int J Mol Sci* **19**: 819–799. <https://doi.org/10.3390/ijms19030779>
- Li HL, Kostulas N, Huang YM, Xiao BG, van der Meide P, Kostulas V, Giedraitis V, Link H (2001) IL-17 and IFN-gamma mRNA expression is increased in the brain and systemically after permanent middle cerebral artery occlusion in the rat. *Neuroimmunol* **116**: 5–14. [https://doi.org/10.1016/s0165-5728\(01\)00264-8](https://doi.org/10.1016/s0165-5728(01)00264-8)
- Liu B, Huang D, Guo Y, Sun X, Chen C, Zhai X, Jin X, Zhu H, Li P, Yu W (2022) Recent advances and perspectives of postoperative neurological disorders in the elderly surgical patients. *CNS Neurosci Ther* **28**: 470–483. <https://doi.org/10.1111/cns.13763>
- Matsumoto Y, La Rose J, Lim M, Adissu HA, Law N, Mao X, Cong F, Mera P, Karsenty G, Goltzman D, Changoor A, Zhang L, Stajkowski M, Grynaps MD, Bergmann C, Rottapel R (2017) Ubiquitin ligase RNF146 coordinates bone dynamics and energy metabolism. *J Clin Invest* **127**: 2612–2625. <https://doi.org/10.1172/jci92233>
- Moller JT, Cluitmans P, Rasmussen LS, Houx P, Rasmussen H, Canet J, Rabbitt P, Jolles J, Larsen K, Hanning CD, Langeron O, Johnson T, Lauen PM, Kris-tensen PA, Biedler A, van Beem H, Fraidakis O, Silverstein JH, Beneken JE, Gravenstein JS (1998) Long-term postoperative cognitive dysfunction in the elderly ISPOCD1 study. ISPOCD investigators. International study of post-operative cognitive dysfunction. *Lancet* **351**: 857–861. [https://doi.org/10.1016/s0140-6736\(97\)07382-0](https://doi.org/10.1016/s0140-6736(97)07382-0)
- Moore KW, de Waal Malefyt R, Coffman RL, O'Garra A (2001) Interleukin-10 and the interleukin-10 receptor. *Annu Rev Immunol* **19**: 683–765. <https://doi.org/10.1146/annurev.immunol.19.1.683>
- Morris R, Kershaw NJ, Babon JJ (2018) The molecular details of cytokine signaling via the JAK/STAT pathway. *Protein Sci* **27**: 1984–2009. <https://doi.org/10.1002/pro.3519>

- Muhammad AS, Muhammad N, Shafiq UR, Noor UL, Tariq A, Metab A, Abdulrahman A, Abdullah F. A (2023) Iron oxide nanoparticles synthesis from madhuca indica plant extract, and assessment of its cytotoxic, antioxidant, anti-inflammatory and anti-diabetic properties via different nano informatics approaches. *ACS Omega*. <https://doi.org/10.1021/acsomega.3c02744>
- Nan H, Chao W, Yuxin Z, Jiying A, Chao Z, Keliang X, Yize L, Haiyun W, Yonghao Y, Guolin W (2016) The role of the Wnt/ β -catenin-Annexin A1 pathway in the process of sevoflurane-induced cognitive dysfunction. *Neurochem* **137**: 240–252. <https://doi.org/10.1111/jnc.13569>
- Nan W, Feng W, Zhe J, Zhen Z, Lian-Kun W, Chun Z, Tao S (2017) Effects of GABA(B) receptors in the insula on recognition memory observed with intel-ligace. *Behav Brain Funct* **13**: 7. <https://doi.org/10.1186/s12993-017-0125-4>
- Naveed M, Bukhari B, Aziz T, Zaib S, Mansoor MA, Khan AA, Shahzad M, Dablood AS, Alrways MW, Almalki AA, Abdulhakeem SA, Majid A (2022) Green synthesis of silver nanoparticles using the plant extract of *Acer oblongifolium* and study of its antibacterial and antiproliferative activity via mathematical approaches. *Molecules* **27**: 4226. <https://doi.org/10.3390/molecules27134226>
- O'Brien H, Mohan H, Hare CO, Reynolds JV, Kenny RA (2017) Mind Over Matter? The hidden epidemic of cognitive dysfunction in the older surgical patient. *Ann Surg* **265**: 677–691. <https://doi.org/10.1097/sla.0000000000001900>
- Qiong M, Hailong Z, Yingning X, Qian H, Xiao L, Wansong Z, Haibing L (2020) NPD1 inhibits excessive autophagy by targeting RNF146 and wnt/ β -catenin pathway in cerebral ischemia-reperfusion injury. *J Recept Signal Transduct Res* **40**: 456–463. <https://doi.org/10.1080/10799893.2020.1756325>
- Shou-Cai Z, Ling-Song M, Zhao-Hu C, Heng X, Wen-Qian W, Fudong L (2017) Regulation of microglial activation in stroke. *Acta Pharmacol Sin* **38**: 445–458. <https://doi.org/10.1038/aps.2016.162>
- Sudheimer KD, O'Hara R, Spiegel D, Powers B, Kraemer HC, Neri E, Weiner M, Hardan A, Hallmayer J, Dhabhar FS (2014) Cortisol, cytokines, and hippo-campal volume interactions in the elderly. *Front Aging Neurosci* **6**: 153. <https://doi.org/10.3389/fnagi.2014.00153>
- van Exel E, Gussekloo J, de Craen AJ, Bootsma-van der Wiel A, Frölich M, Westendorp RG (2002) Inflammation and stroke: the Leiden 85-Plus Study. *Stroke* **33**: 1135–1138. <https://doi.org/10.1161/01.str.0000014206.05597.9e>
- von Rotz RC, Kins S, Hipfel R, von der Kammer H, Nitsch RM (2005) The novel cytosolic RING finger protein dactylidin is up-regulated in brains of patients with Alzheimer's disease. *Eur J Neurosci* **21**: 1289–1298. <https://doi.org/10.1111/j.1460-9568.2005.03977.x>
- Waseem M, Naveed M, Rehman SU, Makhdoom SI, Aziz T, Alharbi M, Alsahamari A, Alasmari AF (2023) Molecular characterization of spa, hld, fmhA, and lukD Genes and computational modeling the multidrug resistance of *Staphylococcus* species through Callindra harrisii silver nanoparticles. *ACS Omega* **8**: 20920–20936. <https://doi.org/10.1021/acsomega.3c01597>
- Xianyi L, Yeru C, Piao Z, Gang C, Youfa Z, Xin Y (2020) The potential mechanism of postoperative cognitive dysfunction in older people. *Exp Gerontol* **130**: 110791. <https://doi.org/10.1016/j.exger.2019.110791>
- Xiaoting W, Kit W, Wenjun O, Sascha Rutz (2019) Targeting IL-10 family cytokines for the treatment of human diseases. *Cold Spring Harb Perspect Biol* **11**. <https://doi.org/10.1101/cshperspect.a028548>
- Xiaoxia Y, Jianhua C, Yubo G, Juan D, Xinli N (2017) Downregulation of Iduna is associated with AIF nuclear translocation in neonatal brain after hypoxia-ischemia. *Neuroscience* **346**: 74–80. <https://doi.org/10.1016/j.neuroscience.2017.01.010>
- Xue-Zhao C, Hong M, Jun-Ke W, Fang L, Bing-Yang W, A-Yong T, Ling-Ling W, Wen-Fei T (2010) Postoperative cognitive deficits and neuroinflammation in the hippocampus triggered by surgical trauma are exacerbated in aged rats. *Prog Neuropsychopharmacol Biol Psychiatry* **34**: 1426–1432. <https://doi.org/10.1016/j.pnpbp.2010.07.027>
- Yeru C, Piao Z, Xianyi L, Huan Z, Jiamin M, Youfa Z, Gang C (2020) Mitophagy impairment is involved in sevoflurane-induced cognitive dysfunction in aged rats. *Aging (Albany NY)* **12**: 17235–17256. <https://doi.org/10.18632/aging.103673>
- Yuanlin D, Zhipeng X, Lining H, Yiyang Z, Zhongcong X (2016) Peripheral surgical wounding may induce cognitive impairment through interleukin-6-dependent mechanisms in aged mice. *Med Gas Res* **6**: 180–186. <https://doi.org/10.4103/2045-9912.196899>
- Yue L, Yiqing Y (2018) Emerging roles of immune cells in postoperative cognitive dysfunction. *Mediators Inflamm* **2018**: 6215350. <https://doi.org/10.1155/2018/6215350>
- Zhichao L, Youzhuang Z, Yihan K, Shangyuan Q, Jun C (2022) Neuroinflammation as the underlying mechanism of postoperative cognitive dysfunction and therapeutic strategies. *Front Cell Neurosci* **16**: 843069. <https://doi.org/10.3389/fncel.2022.843069>
- Zhong-Hong K, Xin C, Hui-Po H, Liang L, Long-Juan L (2017) The oral pretreatment of glycyrrhizin prevents surgery-induced cognitive impairment in aged mice by reducing neuroinflammation and alzheimer's-related pathology via HMGB1 inhibition. *Mol Neurosci* **63**: 385–395. <https://doi.org/10.1007/s12031-017-0989-7>
- Zyad J Carr, Theodore J Cios, Kenneth F Potter, John T Swick (2018) Does dexmedetomidine ameliorate postoperative cognitive dysfunction? a brief review of the recent literature. *Curr Neurol Neurosci Rep* **18**: 64. <https://doi.org/10.1007/s11910-018-0873-z>